Computational Neuroimaging: Maps and Tracts in the Human Brain

Brian A. Wandell and Robert F. Dougherty
Psychology Department and Stanford Institute for Reading and Learning
Stanford University, Stanford, CA 94305

During the last decade, a number of remarkable magnetic resonance imaging (MRI) techniques have been developed for measuring human brain activity and structure. These MRI techniques have been accompanied by the development of signal processing, statistical and visualization methodologies. We review several examples of these methods, drawn mainly from work on the human visual pathways. We provide examples of how two methods- functional MRI (fMRI) and diffusion tensor imaging (DTI) - are used. First, we explain how fMRI enables us to identify and measure several distinct visual field maps and measure how these maps reorganize following disease or injury. Second we explain how DTI enables us to visualize neural structures within the brain's wires (white matter) and measure the patterns of connectivity in individual brains. Throughout, we identify signal processing, statistical, and visualization topics in need of further methodological development.

1. INTRODUCTION

Advances in magnetic resonance imaging (MRI) technology make it possible to obtain a great deal of new information about human brain structure and function. Before the early 1990s, very little information could be obtained about the neural activity in the brain; most of that information was derived from electrical potentials measured at the scalp or positron emission tomography (PET) measurements with fairly coarse resolution and poor signal-to-noise. Magnetic resonance imaging was used principally to measure coarse brain structure, such as the size and shape of large structures.

Then, in the early 90s Ogawa and colleagues discovered MRI methods to measure physiological responses correlated with neural activity (Ogawa et al., 1990). The measurement of functional signals using MRI is called fMRI. Ogawa's specific MR technique, called Blood Oxygen Level Dependent (BOLD) imaging, provides information about the activity in the human brain at a much finer spatial scale than any previous human brain measurement method. The BOLD signals indirectly measure activity localized within the gray matter, where neural computations take place. It is now common to measure activity at a spatial resolution of 3x3x3 mm, and some groups have reported good quality fMRI signals at sub-millimeter resolution. BOLD-fMRI is now used in scientific and clinical experimental work at hundreds of laboratories around the world.

In the late 90s, several groups developed additional MR methods to analyze another important part of the brain: the white matter tracts that form the long-range connections within the brain (Basser et al., 1994; Basser, 1995; Basser and Pierpaoli, 1996; Conturo et al., 1999; Mori et al., 1999; Basser et al., 2000). These experimental measurements extend a conventional MRI technique (diffusion weighted imaging) that measures the rate at which water diffuses in a specific direction. By combining diffusion measurements in many different directions, it is possible to estimate the paths followed by water as it diffuses within the white matter. These "rivers" in the brain generally flow along the major fiber tracts within the white matter. These measurement methods and computational methods, called diffusion tensor imaging (DTI) and fiber tractography (FT), reveal brain structures that were invisible using conventional structural imaging.

All three of these MR measurements- structural MRI, BOLD fMRI and DTI-FT- can be combined in individual human subjects. Because MR is non-invasive and does no harm to the subject, the measurements can also be made to the same subject over time. This permits averaging to improve SNR, or measurements to reveal changes as the brain matures, learns a new skill or undergoes drug or behavioral therapy. Applications of these methods have taught us an enormous amount about the human brain.

Human Vision and Electronic Imaging XI, edited by Bernice E. Rogowitz, Thrasyvoulos N. Pappas, Scott J. Daly,
Proc. of SPIE-IS&T Electronic Imaging, SPIE Vol. 6057, 605701, © 2006 SPIE-IS&T · 0277-786X/06/$15

In Section 2 we describe more about the BOLD signal, with particular attention to what it measures and how BOLD fMRI fits in with other types of brain measurements. We then describe one application of these methods, namely how BOLD fMRI is used to identify important functional units within the visual pathways of individual human subjects, the visual field maps. In Section 3 we describe the basic measurements and algorithms used in DTI-FT. We then describe how these methods are used to identify the fiber tracts that connect the visual pathways in the two hemispheres of individual human brains. In Section 4 we review the general principles of visual organization, and we discuss limitations of the methods that we believe can be lifted by better measurement and computational methods.

2. FUNCTIONAL MRI: MAPS

Neural signals. The cell bodies of neurons in neocortex form a thin (2-4 mm) sheet of tissue. The neuronal sheet contains many folds, allowing it to fit within the skull. When a single hemisphere is flattened, this sheet is roughly the size of an 8.5x11 inch sheet of paper (Wandell et al., 2000; Sincich et al., 2003). Classic MR imaging clearly reveals the shape of the brain and the MR signal intensity can be tuned to provide good contrast between the sheet of gray matter and the white matter fibers that form the core material of the brain (see Figure 1a).

The gray matter neurons are massively interconnected (Braitenberg and Schüz, 1998). Each cubic millimeter of gray matter contains on the order of 50,000 cells, and on average each cell connects to 1000 others. The number of

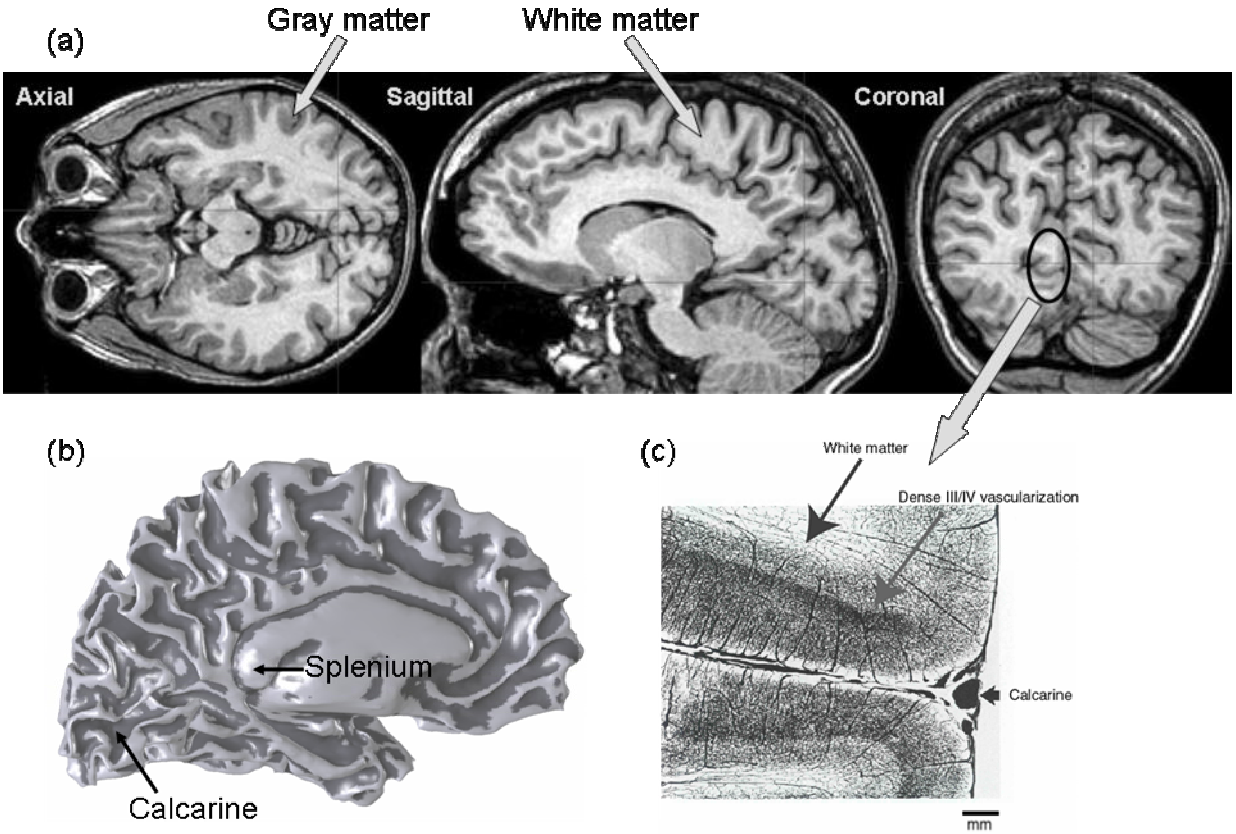

Figure 1. Visualizing structures in the human brain. (a) The neocortical gray matter forms a sheet surrounding the white matter. Three slices are shown and the gray matter and white matter are denoted. The location of left calcarine sulcus is denoted in the coronal view. (b) The gray/white matter boundary is rendered as a surface. The shading indicates the curvature of the surface, with dark indicating sulcus and light gyrus. The 3D surface is smoothed to make permit viewing the depths of the sulci. (c) An zoomed image showing the calcarine vasculature (V1) (Duvernoy et al., 1981).

connections is so abundant that if one were to lay the thin neural processes connecting these cells out in a line, the process within a single cubic millimeter would extend 3-4 kilometers.

Neurons communicate with one another by signals transmitted within a specialized structure, the synapse. Transmission across the very small distance within the synapse takes place via molecules called neurotransmitters. These molecules are released by the pre-synaptic neuron and received by specialized receptors in the post-synaptic neuron. This transmitter initiates a chain of events in the post-synaptic cell, resulting in an analog signal mediated by the modulation of ion-selective channels in the post-synaptic cell. When the analog signal in the post-synaptic neuron reaches a threshold level, the neuron responds by transmitting a brief, discrete electrical pulse, the action potential. The neuron delivering the action potential becomes a pre-synaptic neuron to its outputs. The action potential, carried along the axon, arrives at the pre-synaptic terminal. There it induces transmission of neurotransmitter, beginning the cycle again.

The conduction velocity of an action potential depends primarily on the diameter of the axon: larger axons are generally faster. For very long connections (such as the 150 mm required to connect left and right occipital poles through the corpus callosum), even a large axon of 10 μm diameter requires about 25 ms to conduct an action potential along such a distance (Rushton, 1951; Tolhurst and Lewis, 1992). To reduce these delays, long axons can be wrapped in a fatty myelin sheath. A myelinated axon of the same diameter and length would conduct its signal in less than 3 ms. In fact, most long-range connections in the brain are myelinated, and it is the high lipid content of myelin that makes the white matter appear white. For very short connections, such as those connecting cortical neighbors (<1mm), the benefits of myelin are negligible. Thus, the gray matter contains no myelinated axons. Further, because these short connections between cortical neighbors can be made via small-diameter, unmyelinated axons, many more connections can be packed into a given volume of tissue. Because of this, neighboring cortical regions can be much more densely interconnected than more distant cortical regions.

It is widely believed that the relative sensitivity of each cell to its inputs, coupled with the specific pattern of local connections, combine to perform brain computations. Signals from multiple neurons may add and subtract at these synapses. When the relative sensitivity includes a nonlinear input output relationship, say a logarithmic or exponential function, the neural computations effectively compute products and ratios as well. Steep thresholds and threshold modulations can act as switches and gates. While these general principles seem clear, there are very few cases in which a detailed understanding of a computational function has been analyzed and confirmed for its functional significance.

Over the last forty years, the dominant technique for probing the system properties of neurons in the gray matter has been single-unit physiology. In this method, neuroscientists insert a recording microelectrode and measure the transient action potentials that are carried along the axons. The action potential is a very important stage in the process because it is an essential step when neurons communicate between one another. The action potential, however, is not decisive. While in some cases a single spike from one of the thousand inputs may cause the post-synaptic cell to fire an action potential, this is not common. In many cases a post-synaptic response requires the cumulative input of multiple pre-synaptic cells, within a brief time period, before the post-synaptic cell produces an action potential and delivers it to the next neurons in the chain.

Because cortical neurons communicate by action potentials, and because these potentials can be measured in vivo, much of cortical neuroscience is devoted to theories about the information code by action potentials. Molecular neuroscience has devoted a great deal of time on the molecular mechanisms within the synapse itself, because these transmissions can be influenced by pharmacological agents. For example, the effectiveness of the synaptic transmission process can be modulated by a variety of therapeutic drugs. There are certain parts of the nervous system, such as the retina, where inter-neuron communication is not mediated by spikes. All of the interactions are mediated by analog signals. Hence, retinal physiologists have learned much by studying the analog potentials within that structure.

The BOLD signal. Neuronal signaling is based upon transient changes in the voltage potential across cell membranes, in particular at the pre- and post-synaptic sites. Neural signaling requires energy, and the principal energy consumption is the process of restoring the voltage potentials across the neuronal cell membranes. Significant metabolic energy is required for the ion specific channels to restore the charge balance following the signaling process (Attwell and Laughlin, 2001 ; Lennie, 2003 ; Huettel et al., 2004; Logothetis and Wandell, 2004). The demand for energy causes a

vascular response that increases the arterial blood flow and volume to active regions. The blood supplies oxygen for a glycolytic process that provides the energy used to restore membrane potentials and support neural communication.

The mesh of fine capillaries in the brain (Figure 1a) regulates blood flow on a fine spatial scale that allows sub-millimeter localization of blood flow changes. The increase in the local blood flow and volume, however, takes 4-6 seconds to evolve. Mosso (1881) observed the increase in blood flow in the human brain. The phenomenon was studied in animal models (Roy and Sherrington, 1890) and a particularly interesting human case was described by Fulton (1928).

The MR signal can measure changes in the blood oxygen level (Ogawa and Lee, 1990; Huettel et al., 2004; Logothetis and Wandell, 2004). Such Blood Oxygen Level Dependent (BOLD) imaging is an indirect measure of the local neural activity. Because the local oxygen concentration depends on the energy required to return neurons to their resting state, the BOLD signal does not measure a unique signaling mechanism, such as the number of action potentials or the amplitude of the synaptic potentials. The possibility of dissociation between the BOLD signal and action potentials has been demonstrated experimentally (Lauritzen, 2001). Logothetis' group simultaneously measured action potentials, local field potentials, and BOLD activity (Logothetis, 2002). They found that local field potentials are better correlated with the BOLD signal than action potentials, though both electrical measures correlate with BOLD reasonably well.

In summary, BOLD fMRI indirectly measures neural activity. The neural events detected by the BOLD signal are a combination of those measured by conventional neurophysiological measures. The BOLD signal is not yoked to either action potentials or local field potentials, though it is highly correlated with both. The BOLD signal also depends on the circuitry that combines these signals (see Logothetis and Wandell (2004) for an explanation of the circuit dependence). We do not yet have a complete theoretical model of how the different mechanisms and neural circuitry combine to yield a BOLD response. But, even in the absence of such a model, it is possible to learn a great deal about the brain. The great advantage of the BOLD signal is that it measures the human brain non-invasively at higher spatial resolution than other methods. A disadvantage of the BOLD signal is that it has low temporal resolution because the vascular response develops over time. This combination of properties makes the fMRI BOLD signal well-suited to measuring certain types of neural responses but not others. It is worth noting that the same criticism can be made of any measurement methodology.

Visual field maps. The discovery and characterization of a set of more than a dozen visual field maps in neocortex of macaque and other mammalian species is one of the great advances in visual neuroscience during the last fifty years (Zeki, 1993; Wandell, 1995). These maps are cortical regions whose neurons are organized so that visual stimuli nearby in the visual field are represented by the responses of neurons that are nearby in cortex. Such a spatial arrangement is probably functional- it allows a more dense connectivity between neurons that process neighboring visual field locations than those that process more distant locations. Visual field maps range in size, but they typically span several square centimeters of the cortical surface.

The identification and analysis of functional maps within human visual cortex is one of the most successful applications of BOLD fMRI. Functional imaging is well-suited to measuring the functional brain units of this size. Functional MRI has been used to identify more than ten distinct visual field maps in the human brain, and even more are likely to be identified in the future (Larsson and Heeger, 2005; Swisher et al., 2005). Several but not all of these maps have obvious counterparts in the monkey brain (Zeki, 1969; Essen and Zeki, 1978; Felleman and Essen, 1991).

Primary visual cortex (V1) is the largest and best known visual field map. V1 is the primary recipient zone of retinal signals communicated from the retina via the thalamus (lateral geniculate nucleus) to cortex. V1 is located at the posterior pole of the brain, mostly within the calcarine sulcus, in the occipital lobe. When the V1 map is flattened is occupies a area that is roughly 4 x 8-cm, though the surface area of V1 can differ by a factor of 2.5 between different observers (Dougherty et al., 2003). The V1 map in each hemisphere receives input from retinal neurons with receptive fields in the contralateral visual field, so that left V1 represents the right visual field.

The organization and location of the human visual field map in V1 was originally inferred from visual field losses in patients with lesions. In a classic paper, Horton and Hoyt (Horton and Hoyt, 1991b) summarize their observations as well as related work from the 19th and 20th centuries. FMRI methods for measuring human visual field maps, called

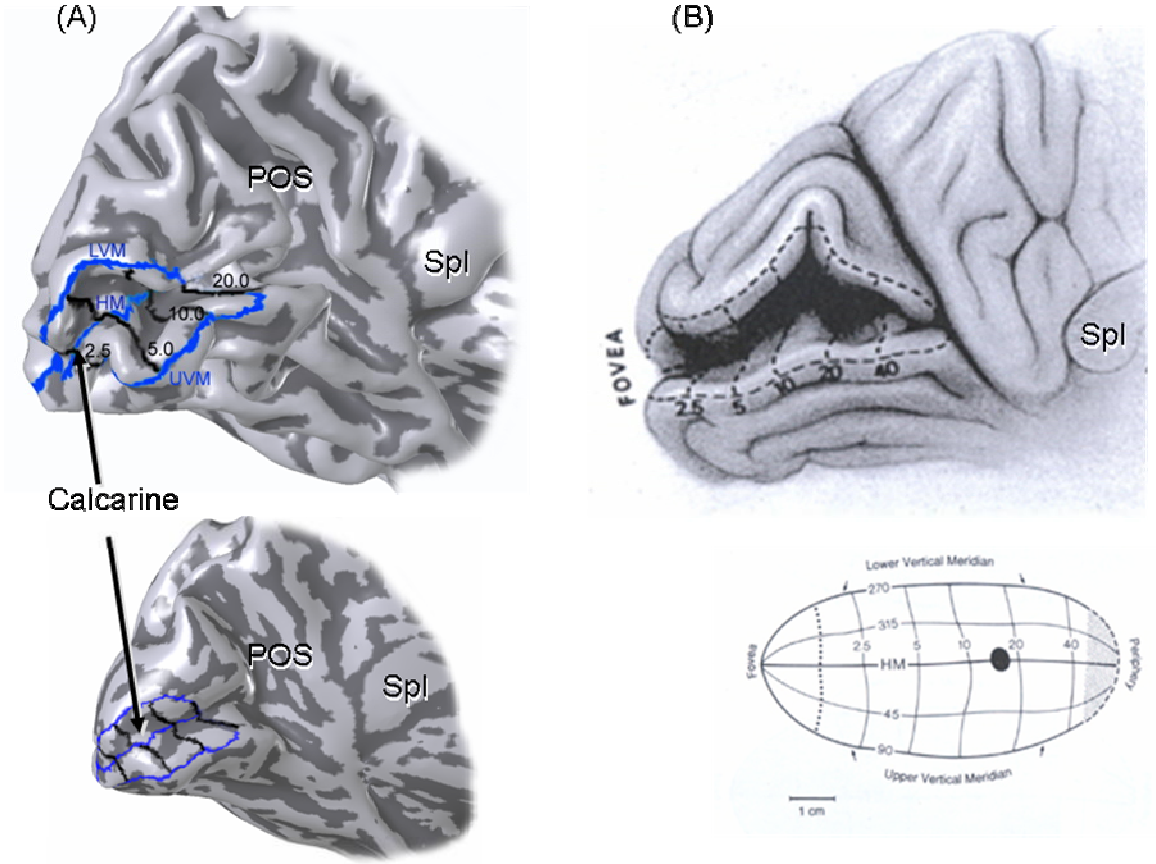

Figure 2. Human V1 visual field maps estimated using fMRI and lesion data agree quantitatively. (A) A visual field map in calcarine, estimated using fMRI, is shown (subject AAB). The black and blue curves are iso-eccentricity (2.5, 5.0, 10 and 20 deg) and meridian lines (LVM = lower vertical meridian, HM = horizontal meridian, and UVM = upper vertical meridian), respectively. The parieto-occipital sulcus (POS) and the splenium (Spl) are indicated. The image represents the surface 0.5 mm above the gray/white matter interface. The same map is shown after smoothing the surface to make the calcarine easier to see. Dark shading indicates a region within a sulcus and light indicates a region on a gyrus. (B) The V1 map estimated from neurological case studies. The upper image shows an artist's rendering of the data on a human brain. The lower image shows a flattened version of calcarine cortex. The black mark in the map denotes the blind spot From (Horton and Hoyt, 1991a).

either traveling-wave or phase-encoded methods, are described in many publications (Engel et al., 1994; Sereno et al., 1995 ; DeYoe et al., 1996; Engel et al., 1997; Wandell, 1999; Wandell et al., 2005). The traveling-wave method measures the map by making two types of measurements. To measure the eccentricity component of the map, a set of annuli contrast patterns is presented in an orderly sequence from fovea to periphery. To measure the angular component, a set of wedge contrast patterns are rotated slowly around the visual field. The eccentricity and angular directions of the stimulus that most effectively drives each cortical location is estimated from the pattern of responses.

The fMRI derived visual field maps, measured in healthy subjects, are in excellent agreement with the maps inferred from the neurological data in patients with lesions (Engel et al., 1997; Wandell, 1999). Both data confirm that when measuring from posterior to anterior in cortex, the visual field representation shifts from the fovea to the periphery (increasing eccentricity). Also, when measuring from the lingual gyrus through the depth of the calcarine sulcus to the cuneus, the visual field representation shifts from the upper vertical meridian through the horizontal meridian to the lower vertical meridian (angle). (See Figure 2.)

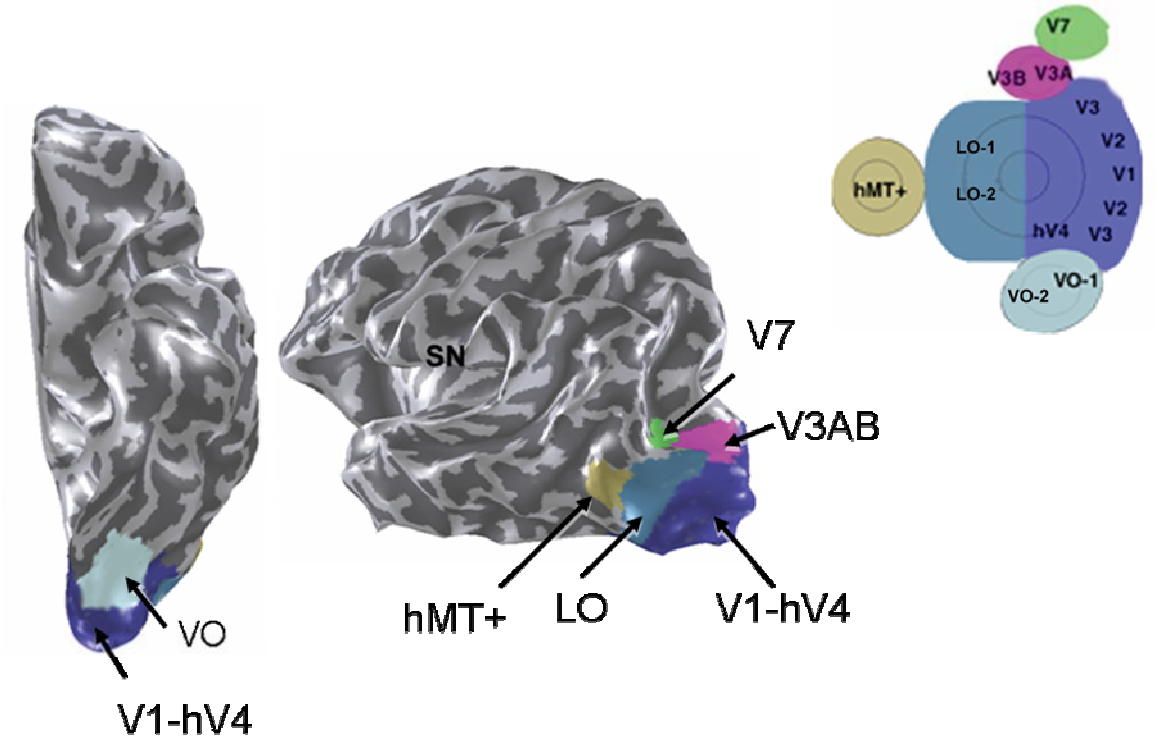

Figure 3. Visual field maps are grouped into clusters. More than ten individual visual field maps are identified in human visual cortex. These maps form clusters that share a confluent fovea with semicircular eccentricity bands, minimizing the length of the synaptic connections required to compare signals originating at common eccentricities. The posterior cluster, including the maps V1, V2, V3 and hV4, is centered on the occipital pole. Clusters were identified on the ventral occipital (VO) portion of the brain, containing at least two maps (Brewer et al., 2005). An additional cluster appears to be located on lateral occipital (LO) (Larsson et al., 2006). This cluster extends towards motion-selective cortex (hMT+) on the anterior-lateral portion of the occipital lobe. Additional maps comprising clusters with their own confluent foveal representations exist on the dorsal surface running along the intra-parietal sulcus (Silver et al., 2005; Swisher et al., 2005). Results are reviewed and the cluster hypothesis introduced in Wandell et al. (2005).

The visual field maps serve as an important coordinate frame for identifying corresponding locations within the brain of different individuals. By measuring the maps in an observer's brain once, it is possible to describe subsequent measurements, say of stimulus responsivity, with respect to these maps. These measurements can be compared with similar measurements in other subjects whose brains may differ in size and folding pattern.

One important open question concerns the functional role of these maps for visual computations. In a series of papers and books, Semir Zeki proposed that individual visual field maps are specialized to carry out discrete visual computations, such as those concerning motion or color (Zeki, 1993). Evidence supporting this view can be found from single unit recordings in macaque; neurons in some maps have very different stimulus selectivity than neurons in other maps. The classic example is direction-selective neurons. While direction-selective neurons are present in V1 and other cortical maps, in MT the vast majority of neurons are direction-selective. These measurements and many others suggest that MT computes visual features associated with stimulus motion. But there is no evidence to support specific functional specializations for most visual field maps. Further, it is not known that MT is the only visual field map that contains a preponderance of direction-selective neurons. Nearby maps (e.g., MST) also contain a high proportion of direction selective cells. There is no reason to believe that neurons in the MT field map are uniquely involved in computing visual motion.

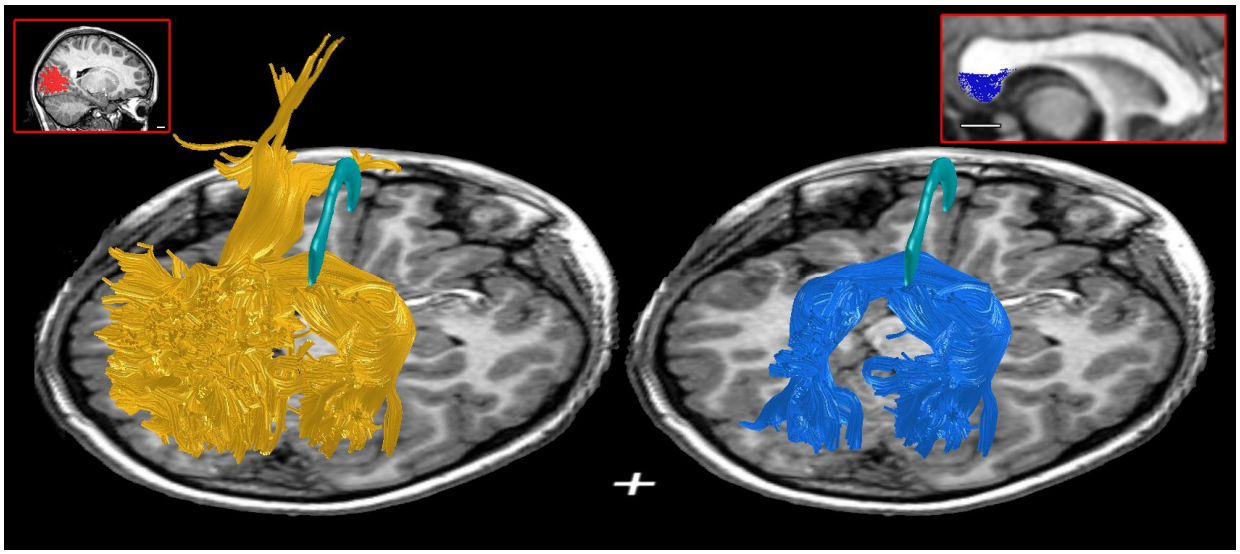

Figure 4. Estimated fiber bundles connecting the occipital lobes. In this example, fiber tracts are estimated from seed points in the occipital lobe of the left hemisphere (upper left inset) to find all fiber bundles that pass through the left occipital lobe (yellow fibers in the left image). The subset of occipital lobe fibers that pass through the corpus callosum (shown in cyan) is shown in the right image (blue fibers). The location of these fibers in the plane of the corpus callosum is shown in the upper right inset. Scale bars indicate 1 cm. From (Dougherty et al., 2005), Figure 1.

As an alternative, we porposed that clusters of maps may form the basic functional unit for visual computations (Wandell et al., 2005). On this view, the collection of maps in VO may be specialized to interpret form, while the maps near hMT+ may be specialized for motion. The maps themselves may function as integrated units to derive critical stimulus features and signal these properties to other portions of cortex. This is a very speculative idea that requires a great deal of additional experimental work. But it is useful to have an alternative hypothesis to the notion that functional specialization is uniquely associated with individual maps. (See Figure 3.)

DIFFUSION TENSOR IMAGING: TRACTS

Long-range connections form early (well before birth) and are likely to be programmed genetically, rather than by experience. The long-range connectivity establishes cortical modularity (e.g., see Sur and Leamey, 2001). For example, primary visual cortex forms in the calcarine sulcus because that is where the optic radiations terminate. If the genetic program for an individual could be altered to re-target all the connections to and from primary visual cortex to a different cortical region, then that region would become primary visual cortex. Thus, measuring the long-range connectivity of the brain is an essential step toward a complete understanding of brain function.

The long-range connectivity is also crucial for understanding brain development. While existing connections can be pruned away or strengthened, new long-range connections do not form in the brain once it is myelinated (Horner and Gage, 2000). The exuberant connectivity present in very young brains (Bourgeois and Rakic, 1993) allows them to better tune their structure with experience and adapt to damage. But, as these connections are pruned away during development, they can never be recovered, thus limiting adult plasticity. Also, while the young brain is over-connected, it is not fully connected; thus, the genetically-determined connectivity imposes limits to plasticity at any age. Finally, the details of this genetically-programmed connectivity pattern are likely to be polymorphic and thus vary from person to person. The variability in this connectivity pattern could very well be the defining feature for many heritable psychological traits and disorders (e.g., Hannula-Jouppi et al., 2005).

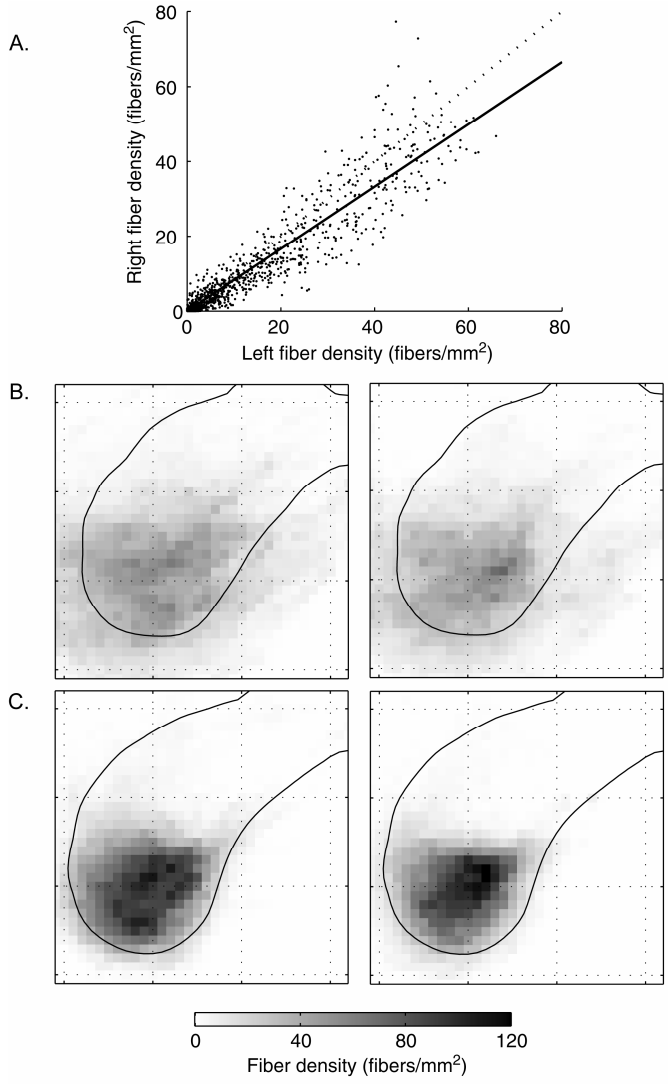

Figure 5. Convergence of occipital-callosal fiber bundle densities estimated independently in left and right hemispheres. The data from 53 children were combined. (A) The data from each child was translated and scaled into a common coordinate frame, aligned with the AC-PC axis. The graph compares the number of fiber bundles per square millimeter (per subject) from the left (horizontal axis) and right (vertical axis) at locations within a grid drawn in the corpus callosum. (B) The images show the fiber bundle density estimates overlaid on a contour that represents the average splenium in AC-PC aligned coordinates. These data form the basis of the graph in panel (A). The two images show the spatial distribution of the fibers derived from the left (left panel) and right (right panel) occipital lobes. (C) The data from each child was translated in two dimensions so that the combined center-of-mass of left and right occipital-callosal fiber bundles is at a common location. This translation reduces the variance caused by errors in registering the brains. Grid lines are spaced at 5 mm. From (Dougherty et al., 2005), Figure 3.

Surprisingly, it is difficult to measure the organization and properties of the white matter tracts in the living human brain. Conventional anatomical measurements show the white matter as a homogeneous object with very little structure. Hence, the development of magnetic resonance methods for identifying these tracts in the living brain has opened up new possibilities for understanding how brain development and these important brain structures co-vary with human behavior and health.

The MR methods for discovering the white matter tracts form and properties are again indirect measures. This time the MR methods take advantage of the relationship between diffusion and cellular structure. Magnetic resonance imaging (MRI) has long had pulse sequences available for estimating the mean distance of diffusion in a single direction. Diffusion weighted (DW) imaging is commonly used in clinical practice to identify ischemia. This imaging modality uses the motion of water molecules to probe the cellular and molecular structures at a resolution much finer than the image resolution. In current clinical practice, DW measurements are made in three directions and the results are summarized by three DW images (e.g., coronal, axial and sagittal).

In the mid-90s mathematicians and neuroscientists developed powerful computational methods to integrate diffusion data acquired in more than three directions (Basser et al., 1994). These methods, called Diffusion Tensor Imaging (DTI), use multiple (usually six or more) DW images. The measurements are summarized using a 3-dimensional Gaussian model of diffusion- a tensor (ellipsoid) that approximates how far the water molecules diffuse in all directions from a point. The diffusion tensor provides a much better summary of the cellular and molecular properties than the three separate DW images.

In the late-90s, further computational advances permitted scientists to use whole brain data sets of diffusion tensors to deduce basic organization of white matter fiber bundles. The myelin sheath that covers the long-range axons in the white matter impedes water diffusion. This causes water to diffuse more easily along the length of axon bundles and impedes diffusion orthogonal to the bundles. Thus, the diffusion measurements

in the white matter provide information about the local orientation of these fiber bundles. Computational algorithms were developed to link tensors that share similar principal diffusion directions and thus estimate the fiber bundle pathways (see Mori and van Zijl, 2002 and Bammer et al., 2003 for reviews). The combination of DTI and fiber tracking (FT) produces estimates of the major fiber bundles in the brain of individual subjects. The shapes and properties of these fiber tracts, as well as their destinations in cortex, can be estimated.
Our group has developed tools for visually exploring DTI-FT estimates (Akers et al., 2004; Sherbondy et al., 2005) and for evaluating the quality of the tract estimates (Dougherty et al., 2005). Figure 4 shows estimates of the fiber tracts that connect the two occipital lobes in an individual subject's brain (an 11-year old child). By estimating these fiber tracts independently from the left and right occipital lobes in each subject, we can get a measure of the quality of the current DTI-FT methods (Figure 5). These independent fiber tract estimates originating from the two hemispheres converge onto a common region in the lower half of the splenium (the posterior corpus callosum). This observation validates the basic DTI-FT methodology. However, in any individual brain, we can find some fiber tract estimates that are clearly errors. The fiber tracts most prone to error are those that inter-digitate with other fiber tracts oriented in a different direction. This "crossing-fiber" problem is a serious limitation of the current DTI-FT methods. Various groups are developing methods to solve this problem by fitting more complex diffusion models (Tuch, 2004; Hosey et al., 2005; Parker and Alexander, 2005). A full solution to the problem will also likely involve innovations in the fiber-tracking algorithms that combine the diffusion measurements at each voxel (e.g., by introducing prior anatomical knowledge).

Diffusion imaging can also be used to compare white matter structure between individual brains and between groups of individuals. Group differences in white matter structure have been reported in various disorders, including schizophrenia (Kubicki et al., 2005), multiple sclerosis (Bammer et al., 2000), epilepsy (Diehl et al., 2005), and reading disability (Klingberg et al., 2000; Beaulieu et al., 2005; Deutsch et al., 2005). The majority of group comparisons using DTI data involve a scalar value derived from the diffusion tensor, such as the mean diffusivity or the fractional anisotropy (the normalized variance of the eigenvalues of the tensor). This fact is partly due to the lack of statistical tools necessary to draw inferences from a tensor field. To address this limitation, we have developed statistical methods for comparing the principal diffusion direction between groups of brains (Schwartzman et al., 2005). We are also developing methods that allow statistical comparisons between the full tensors (Schwartzman et al., 2005).

4. DISCUSSION

The last fifteen years have produced an unprecedented growth in the ability to measure structure and function in the human brain. It is possible to coordinate FMRI and DTI measurements with behavior and different disease states. Because fMRI and DTI signals have good signal-to-noise in individual subjects, the methods are useful for diagnosis and monitoring therapeutic treatments.

The MR measurements are complementary to many other sources of information about the brain. While the MR technologies make fairly high spatial resolution measurements, they cannot follow rapid changes in brain state. Rapid events can be detected using scalp recordings of electrical (EEG) and magnetic (MEG) fields, and there are attempts to coordinate these measurements (Dale et al., 2000; Babajani et al., 2005). When different measurement modalities depend on the same biological signals (e.g., post-synaptic potentials), taking advantage of spatial and temporal resolution is possible. But, there is reason to be concerned about the commonality of the underlying mechanisms. It is widely thought that EEG and MEG depend on the responses of the large pyramidal neurons that make up 85% of all cortical neurons (Braitenberg and Schüz, 1998). The fMRI responses depend upon the total metabolic energy, however, and there is no data to suggest that these neurons consume 85% of the metabolic energy, and experimental conditions exist that dissociate the responses of large neurons and blood flow (Mathiesen et al., 1998). At this time we cannot be certain that fMRI and EEG or MEG measure the same neural signals, and this limits our ability to link data obtained from the these methods (Wandell and Wade, 2003). Integration of the information from different measurement methods can only be secure after we develop a better understanding of the neural mechanisms that give rise to the different neuroimaging signals.

Going forward, we think there are many opportunities for improving both data acquisition methods and software tools. Some of these opportunities are related to software: Databases for coding and sharing information are in a very primitive state. Current software analysis tools used in the scientific labs are oriented towards group comparisons rather

than single-subject analysis, so that there are important needs to develop software technologies geared for single subject analyses. The next few years will see a substantial opportunity to combine information about genomics with neuroimaging data (Rueda et al., 2005). Advances in MR-spectroscopy and the ability to easily obtain genetic information will make it possible to build a much more complete view of the brain, its development and function. The engineering and medical infrastructure needed to integrate this information and build a coherent picture is an exciting and challenging task that awaits us.

ACKNOWLEDGMENTS

We thank David Akers, Alyssa Brewer, Michal Ben-Shachar, Guillaume Bertello, Sing Cheung, Gayle Deutsch, Serge Dumoulin, Glen Fox, Arvel Hernandez, Junjie Liu, David Ress, Rory Sayres, Armin Schwartzmannm, Anthony Sherbondy for scientific discussions and their work on data analysis. We thank Roland Bammer and Gary Glover for assistance in obtaining MR measurements. We thank Jan Ruby for administrative help. Supported by EY-03164 and EY-015000.

5. REFERENCES

Akers D, Sherbondy A, Mackenzie R, Dougherty R, Wandell B (2004) Exploration of the Brain's White Matter Neural Pathways with Dynamic Queries. Proceedings of IEEE Visualization:377-384.

Attwell D, Laughlin SB (2001) An energy budget for signaling in the grey matter of the brain. J Cereb Blood Flow Metab 21:1133-1145.

Babajani A, Nekooei MH, Soltanian-Zadeh H (2005) Integrated MEG and fMRI model: synthesis and analysis. Brain Topogr 18:101-113.

Bammer R, Acar B, Moseley ME (2003) In vivo MR tractography using diffusion imaging. Eur J Radiol 45:223-234.

Bammer R, Augustin M, Strasser-Fuchs S, Seifert T, Kapeller P, Stollberger R, Ebner F, Hartung HP, Fazekas F (2000) Magnetic resonance diffusion tensor imaging for characterizing diffuse and focal white matter abnormalities in multiple sclerosis. Magn Reson Med 44:583-591.

Basser PJ (1995) Inferring microstructural features and the physiological state of tissues from diffusion-weighted images. NMR Biomed 8:333-344.

Basser PJ, Pierpaoli C (1996) Microstructural and physiological features of tissues elucidated by quantitative-diffusion-tensor MRI. J Magn Reson B 111:209-219.

Basser PJ, Mattiello J, LeBihan D (1994) MR diffusion tensor spectroscopy and imaging. Biophys J 66:259-267.

Basser PJ, Pajevic S, Pierpaoli C, Duda J, Aldroubi A (2000) In vivo fiber tractography using DT-MRI data. Magn Reson Med 44:625-632.

Beaulieu C, Plewes C, Paulson LA, Roy D, Snook L, Concha L, Phillips L (2005) Imaging brain connectivity in children with diverse reading ability. Neuroimage 25:1266-1271.

Bourgeois J, Rakic P (1993) Changes of synaptic density in the primary visual cortex of the macaque monkey from fetal to adult stage. J Neurosci 13:2801-2820.

Braitenberg V, Schüz A (1998) Cortex: Statistics and Geometry of Neuronal Connectivity, 2nd Edition.

Brewer AA, Liu J, Wade AR, Wandell BA (2005) Visual field maps and stimulus selectivity in human ventral occipital cortex. Nat Neurosci 8:1102-1109.

Conturo TE, Lori NF, Cull TS, Akbudak E, Snyder AZ, Shimony JS, McKinstry RC, Burton H, Raichle ME (1999) Tracking neuronal fiber pathways in the living human brain. Proc Natl Acad Sci U S A 96:10422-10427.

Dale AM, Liu AK, Fischl BR, Buckner RL, Belliveau JW, Lewine JD, Halgren E (2000) Dynamic statistical parametric mapping: combining fMRI and MEG for high-resolution imaging of cortical activity. Neuron 26:55-67.

Deutsch GK, Dougherty RF, Bammer R, Siok WT, Gabrieli JD, Wandell B (2005) Children's reading performance is correlated with white matter structure measured by diffusion tensor imaging. Cortex 41:354-363.

DeYoe EA, Carman GJ, Bandettini P, Glickman S, Wieser J, Cox R, Miller D, Neitz J (1996) Mapping striate and extrastriate visual areas in human cerebral cortex. Proc Natl Acad Sci (USA) 93:2382-2386.

Diehl B, Symms MR, Boulby PA, Salmenpera T, Wheeler-Kingshott CA, Barker GJ, Duncan JS (2005) Postictal diffusion tensor imaging. Epilepsy Res 65:137-146.

Dougherty RF, Ben-Shachar M, Bammer R, Brewer AA, Wandell BA (2005) Functional organization of human occipital-callosal fiber tracts. Proc Natl Acad Sci U S A 102:7350-7355.
Dougherty RF, Koch VM, Brewer AA, Fischer B, Modersitzki J, Wandell BA (2003) Visual field representations and locations of visual areas V1/2/3 in human visual cortex. J Vis 3:586-598.
Duvernoy H, Delon S, Vannson J (1981) Cortical blood vessels of the human brain. Brain Res Bull 7:519–579.
Engel SA, Glover GH, Wandell BA (1997) Retinotopic organization in human visual cortex and the spatial precision of functional MRI. Cereb Cortex 7:181-192.
Engel SA, Rumelhart DE, Wandell BA, Lee AT, Glover GH, Chichilnisky EJ, Shadlen MN (1994) fMRI of human visual cortex. Nature 369:525.
Essen DCV, Zeki SM (1978) The topographic organization of rhesus monkey prestriate cortex. J Physiol 277:193-226.
Felleman DJ, Essen DCV (1991) Distributed hierarchical processing in the primate cerebral cortex. Cerebral Cortex 1:1-47.
Fulton JF (1928) Observations upon the vascularity of the human occipital lobe during visual activity. Brain 51:310-320.
Hannula-Jouppi K, Kaminen-Ahola N, Taipale M, Eklund R, Nopola-Hemmi J, Kaariainen H, Kere J (2005) The Axon Guidance Receptor Gene ROBO1 Is a Candidate Gene for Developmental Dyslexia. PLoS Genet 1:e50.
Horner PJ, Gage FH (2000) Regenerating the damaged central nervous system. Nature 407:963-970.
Horton J, Hoyt W (1991a) The representation of the visual field in human striate cortex. Arhives of Opthalmology 109:816-824.
Horton JC, Hoyt WF (1991b) The representation of the visual field in human striate cortex. A revision of the classic Holmes map. Arch Ophthalmol 109:816-824.
Hosey T, Williams G, Ansorge R (2005) Inference of multiple fiber orientations in high angular resolution diffusion imaging. Magn Reson Med 54:1480-1489.
Huettel S, Song A, McCarthy G (2004) Functional magnetic resonance imaging. Sunderland, Mass: Sinauer Associates.
Klingberg T, Hedehus M, Temple E, Salz T, Gabrieli JD, Moseley ME, Poldrack RA (2000) Microstructure of temporo-parietal white matter as a basis for reading ability: evidence from diffusion tensor magnetic resonance imaging. Neuron 25:493-500.
Kubicki M, McCarley R, Westin CF, Park HJ, Maier S, Kikinis R, Jolesz FA, Shenton ME (2005) A review of diffusion tensor imaging studies in schizophrenia. J Psychiatr Res.
Larsson J, Heeger DJ (2005) HUMAN VISUAL CORTEX BETWEEN DORSAL V3 AND V5/MT+ CONTAINS TWO COMPLETE MAPS OF THE CONTRALATERAL VISUAL HEMIFIELD. In: Society for Neuroscience. Washington, DC:: Society for Neuroscience.
Larsson J, Landy MS, Heeger DJ (2006) Orientation-selective adaptation to first- and second-order patterns in human visual cortex. J Neurophysiol 95:862-881.
Lauritzen M (2001) Relationship of spikes, synaptic activity, and local changes of cerebral blood flow. J Cereb Blood Flow Metab 21:1367-1383.
Lennie P (2003) The cost of cortical computation. Curr Biol 13:493-497.
Logothetis NK (2002) The neural basis of the BOLD fMRI signal. Philosophical Transactions of the Royal Society Series B (London) 357:1003-1037.
Logothetis NK, Wandell BA (2004) Interpreting the BOLD signal. Annu Rev Physiol 66:735-769.
Mathiesen C, Caesar K, Akgoren N, Lauritzen M (1998) Modification of activity-dependent increases of cerebral blood flow by excitatory synaptic activity and spikes in rat cerebellar cortex. J Physiol 512:555-566.
Mori S, van Zijl PC (2002) Fiber tracking: principles and strategies - a technical review. NMR Biomed 15:468-480.
Mori S, Crain BJ, Chacko VP, van Zijl PC (1999) Three-dimensional tracking of axonal projections in the brain by magnetic resonance imaging. Ann Neurol 45:265-269.
Mosso A (1881) Ueber den Kreislauf des Blutes im Menschlichen Gehirn. Leipzig: Verlag von Veit & Company.
Ogawa S, Lee TM (1990) Magnetic resonance imaging of blood vessels at high fields: in vivo and in vitro measurements and image simulation. Magn Reson Med 16:9-18.
Ogawa S, Lee TM, Kay AR, Tank DW (1990) Brain magnetic resonance imaging with contrast dependent on blood oxygenation. Proc Natl Acad Sci U S A 87:9868-9872.
Parker GJ, Alexander DC (2005) Probabilistic anatomical connectivity derived from the microscopic persistent angular structure of cerebral tissue. Philos Trans R Soc Lond B Biol Sci 360:893-902.
Roy CS, Sherrington CS (1890) On the regulation of the blood supply of the brain. JPhysiol(Lond) 11:85-108.

Rueda MR, Rothbart MK, McCandliss BD, Saccomanno L, Posner MI (2005) Training, maturation, and genetic influences on the development of executive attention. Proc Natl Acad Sci U S A 102:14931-14936.
Rushton WA (1951) A theory of the effects of fibre size in medullated nerve. J Physiol 115:101-122.
Schwartzman A, Dougherty RF, Taylor JE (2005) Cross-subject comparison of principal diffusion direction maps. Magn Reson Med 53:1423-1431.
Sereno MI, Dale AM, Reppas JB, Kwong KK, Belliveau JW, Brady TJ, Rosen BR, Tootell RB (1995) Borders of multiple human visual areas in humans revealed by functional mri. Science 268:889-893.
Sherbondy A, Akers D, Mackenzie R, Dougherty R, Wandell B (2005) Exploring connectivity of the brain's white matter with dynamic queries. IEEE Trans Vis Comput Graph 11:419-430.
Silver MA, Ress D, Heeger DJ (2005) Topographic maps of visual spatial attention in human parietal cortex. J Neurophysiol 94:1358-1371.
Sincich LC, Adams DL, Horton JC (2003) Complete flatmounting of the macaque cerebral cortex. Vis Neurosci 20:663-686.
Sur M, Leamey CA (2001) Development and plasticity of cortical areas and networks. Nat Rev Neurosci 2:251-262.
Swisher JD, Crum KE, McMains SA, Halko MA, Sheremata SL, Somers DC (2005) Stimulus-driven retinotopic maps in human parietal cortex observed via fmri. In. Washington, DC: Society for Neuroscience.
Tolhurst DJ, Lewis PR (1992) Effect of myelination on the conduction velocity of optic nerve fibres. Ophthalmic Physiol Opt 12:241-243.
Tuch DS (2004) Q-ball imaging. Magn Reson Med 52:1358-1372.
Wandell BA (1995) Foundations of Vision. Sunderland, MA: Sinauer Press.
Wandell BA (1999) Computational neuroimaging of human visual cortex. Annual Review of Neuroscience 22:145-173.
Wandell BA, Wade AR (2003) Functional imaging of the visual pathways. Neurol Clin 21:417-443, vi.
Wandell BA, Chial S, Backus BT (2000) Visualization and measurement of the cortical surface. Journal of Cognitive Neuroscience 12:739-752.
Wandell BA, Brewer AA, Dougherty RF (2005) Visual field map clusters in human cortex. Philos Trans R Soc Lond B Biol Sci 360:693-707.
Zeki S (1993) A Vision of the Brain. London: Blackwell Scientific Publications.
Zeki SM (1969) Representation of central visual fields in prestriate cortex of monkey. Brain Research 14:271-291.